Journal of Mechanical and Electrical Intelligent System (JMEIS)

Developing and applying 2-step learning for analysis of glomerular epithelial cell images

Yusuke Ono[1,a], Tsutomu Matsuura[1,b], Toshiyuki Matsuzaki[2,c], Keiju Hiromura[2,d] and Takeo Aoki[3,e]

[1]Graduate School of Science and Technology, Gunma University, 29-1 Hon-cho, Ota, Gunma 373-0057, Japan

[2]Graduate School of Medicine, Gunma University, 3-39-22 Showa-machi, Maebashi, Gunma 371-8511, Japan

[3]Gunma Prefectural College of Health Sciences, 323-1 Kamioki-machi, Maebashi, Gunma 371-0052, Japan

[a]<t182b001@gunma-u.ac.jp>, [b]<matsuura@gunma-u.ac.jp>, [c]<matoshi@gunma-u.ac.jp>, [d]<hiromura@gunma-u.ac.jp>, [e]<aoki-take@gch.ac.jp>

Keywords: glomerular epithelial cell, fisher vector, support vector machine, 2-step learning

Abstract. We have the impression that glomerular epithelial cells are bloating and changing in shape with kidney disease progress. However, these views are only from subjective observations, and so we need to have an objective basis such as statistical method. To obtain this basis, we prepared SEM images of glomerular epithelial cells which are taken from five types of mice of each disease stage. We divide these images into three groups with a relatively similar tendency. Our target is to quantify these changes by classifying these groups with high accuracy. In this paper, we propose the new method "2-step learning" for the classification with high accuracy and apply it for our dataset. So, we should validate the effectiveness of our method. As a result of our investigation, the accuracy of our method achieved 78.5%, and it is 12.6% higher than previous research. Furthermore, we confirmed the generalization ability of our method.

1. Introduction

Glomerular cell exists in kidney and has the function of filtering the blood and removing waste products. Glomerular epithelial cell is epithelial tissue of glomerulus that contains three parts: cell body, major process and foot process. The SEM image of a sample of the cell is shown in Fig.1. In previous research [1], researchers judge the cell that is normal or abnormal from the foot process effacement appeared by the molecular structure changes of slit membrane. On the other hand, observing the SEM images of glomerular epithelial cells, we have the impression that foot processes are bloating and changing in shape with kidney disease progress. A sample of foot process image is shown in Fig.2 Left. We think that we would like to apply this characteristic for quantifying disease progress and aiding the diagnosis. However, these views are only from subjective observations, and so we need to have an objective basis such as statistical method. According to the previous research [2] in the region of cell body, it quantified the progress by using morphological features, however, it has the problem that includes a subjective judgement in parameter setting. We focus on regions of foot process that obtained from each disease stage, and we classify them with high accuracy by a machine learning method. This result will lead to quantify the progress of disease and diagnose it with the exclusion of subjectivity. Recently we reported in [3] that we achieved the accuracy of 65.9% by using feature regions and Fisher Vector. It is hard to say that the accuracy of our method is enough, and so we should improve it. Therefore, in this paper, our aim is to propose the new method "2-step learning"

for classifying disease stages with high accuracy by glomerular epithelial cell images and validate the effectiveness of it.

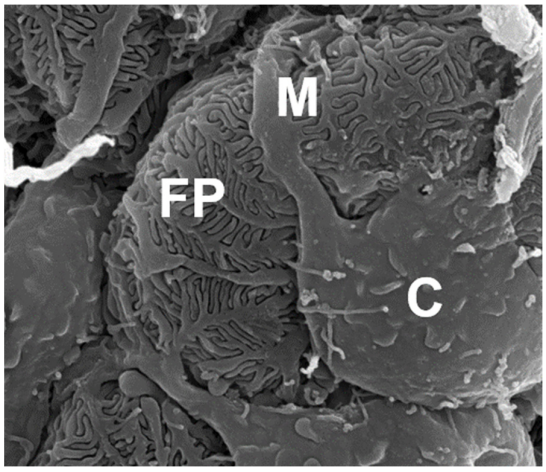

Fig.1. Glomerular epithelial cell C: cell body, M: major process, FP: foot process

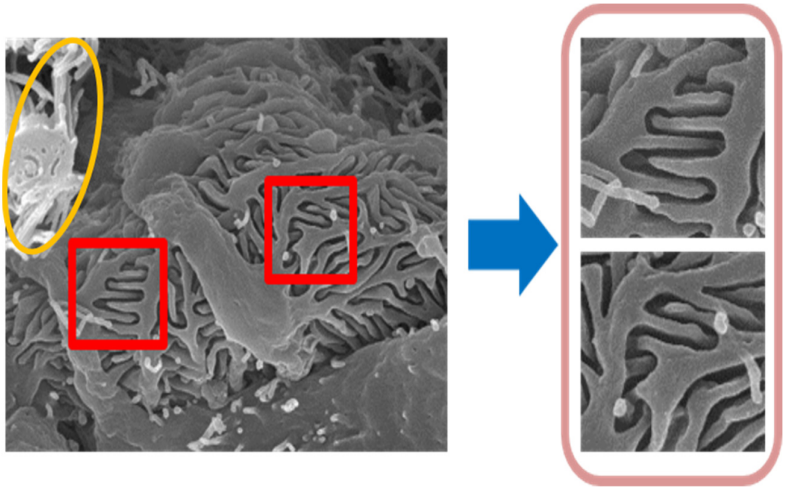

Fig. 2. Extraction of Feature Region images, Left: Original image (FP), Right: Feature Region Images; FRI

2. Image data to be analyzed

We prepared five types of mice that are wild type, wild type with diabetes, old type, mutant type and mutant type with diabetes. We took images of foot process regions from them by SEM (HITACHI S-800), and we set parameters as follows: the magnification of 13000, imaging area is 79[μm] × 93[μm], image size is 1890[px] × 2228[px].

Each type of mouse is prepared as follows. Wild type mice are C57BL/6. Mutant type mice are knock-in mouse (C57BL/6 background) with the deleted intracellular domain of Signal Regulatory Protein α (SIRPα) that made for the investigation of the role of SIRPα expression on glomerular epithelial cell [10]. Mice with diabetes are created by next process. The streptozotocin with 50 [mg/kg] which destroys pancreatic islet β cells specifically and causes the diabetes mellitus type 1 is dissolved in physiological saline. We administered it to intraperitoneal of mice with five consecutive days, and

we use mice that achieved the blood glucose level over 300 [mg/dl] after two weeks. These image data are provided by Prof. Aoki which belongs to Gunma Prefectural College of Health Sciences.

However, we have the problem which the number of our images is few for applying the machine learning. Thus, we divide five types into three classes with a relatively similar tendency based on medical viewing, and we classify them. Grouping and the number of each class is shown in Table 1.

Table 1 Grouping and the number of each image

Class	Type	Number of Original	Number of FRI
Group1	wild type	96	447
Group2	wild type with diabetes aged type	193	922
Group3	mutant type mutant type with diabetes	167	678

3. About 2-step learning

We had thought feature regions express features of each group that captured an engagement area such as Fig.2 Right. However, we achieved the accuracy of classification in about 50 to 60% by using those images of the groups in previous research [3]. When we observed the whole image such as Fig.2, we knew that shapes of feature regions captured by auto-extraction method [4] are variety. So, the previous classification had low accuracy because the characteristic of other classes exists. The classifiers should be learned from not only feature region images but also all over images. Therefore, we propose 2-step learning method that learns features in two steps. In the 1st step, we extract features from feature region images and learn the rough background knowledge. In the 2nd step, we obtain more detailed information by scanning and learning the whole original images with the background knowledge learned in the 1st step.

In Figs. 3-5, we show the outline of two steps.

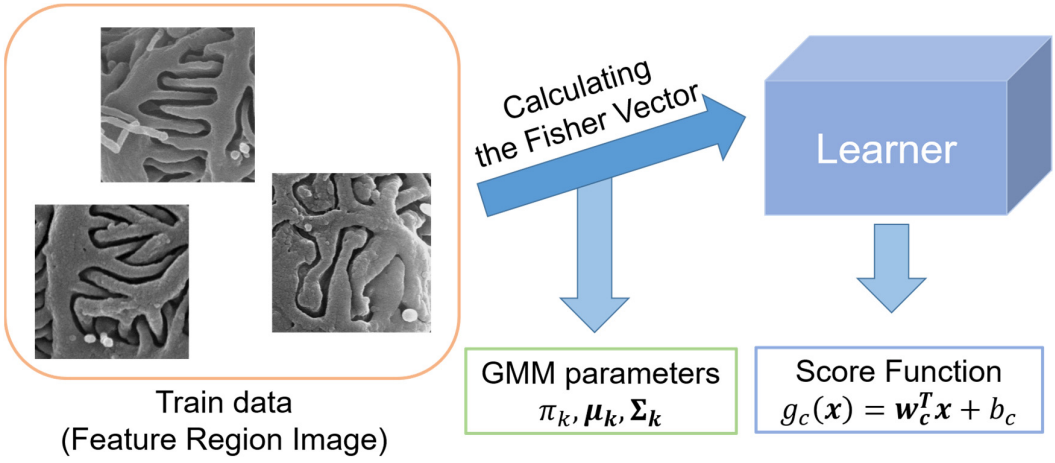

Fig. 3. Learning Feature Region Images in the 1st step

In the 1st step, we extract the Fisher Vector from feature region images that obtained by auto-extraction method using template-matching and learn them by linear-SVM, thereby obtaining score functions for each class. The details of the Fisher Vector are described in [5] and Appendix. We apply One vs Rest for expanding to multi class SVM. At this time, for calculating the Fisher Vector in next step, we obtain GMM parameters: π, μ, Σ. The details of GMM are described in [8].

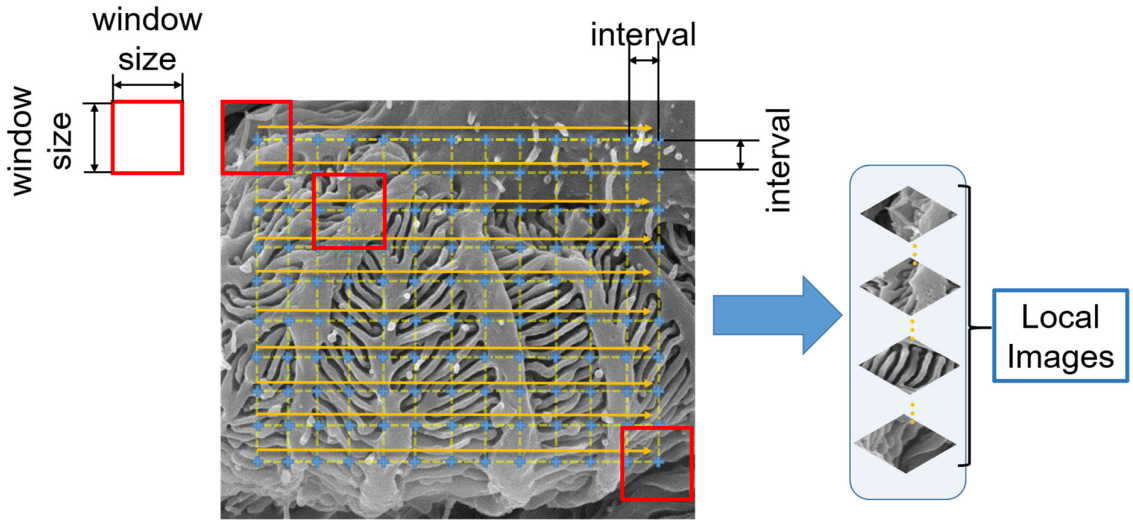

Fig. 4. Scanning the whole original image and obtaining local images in the 2nd step

In the 2nd step, we scan the whole original image for obtaining local images. In this scanning, window size and interval are arbitrarily determined.

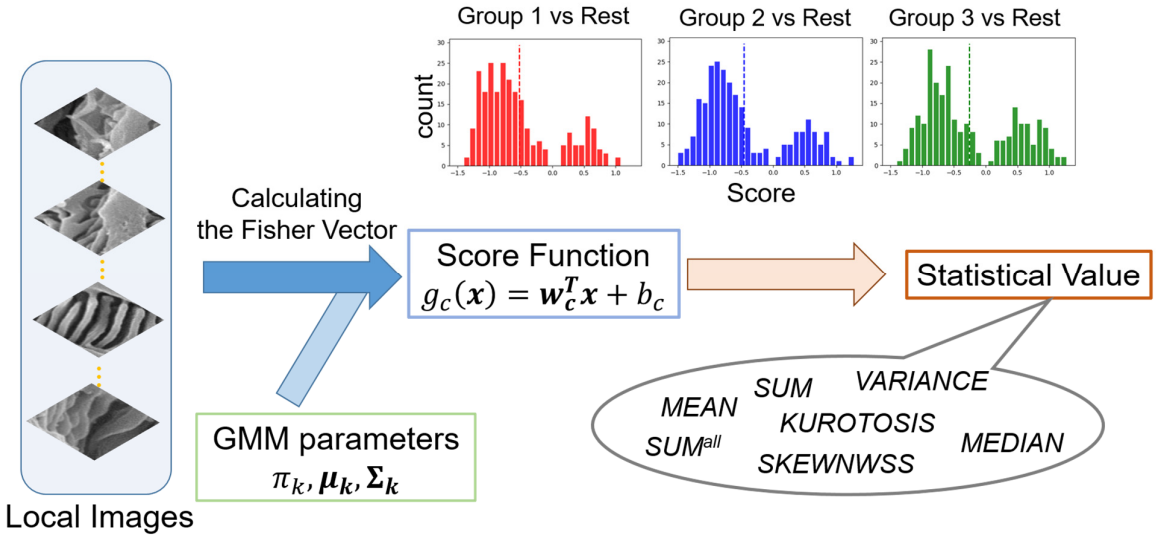

Fig. 5. Creating score-distribution from local images in the 2nd step

We calculate score-distribution from local images. Score value of these images are obtained by the Fisher Vector which calculated by GMM parameters in the 1st step and score functions for each class. Then, we calculate the statistical value from these score-distribution. The statistical value has features of 7 types: total, average, variance, kurtosis, skewness and median for each class, and total of all classes. Finally, we classify them by learning these statistical features using linear-SVM.

Here, we decide parameters for 2-step learning as follows: the window size is 511[px]×511[px] and the interval is 100[px]. In addition, we decide parameters of SIFT and GMM as the Fisher Vector parameters used in our method. The details of SIFT are described in [6, 7]. We use gridded points for feature description of SIFT. The description area is prepared 3 types: 11[px]×11[px], 31[px]×31[px],

and 51[px]×51[px]. The interval of gridded points is 10[px]. The number of components for GMM is 32 on basis of AIC and the rule of thumb. For calculated the Fisher Vector, we apply L2 normalize and Power normalize of $\alpha = 0.3$. Furthermore, we use linear-SVM applied One vs Rest for the final identification.

4. Validating the effectiveness of 2-step learning

We validate the effectiveness of our method for glomerular epithelial cell images by two ways as follows. First, we compare our new method with previous one. Second, we investigate the generalization ability of our method.

4.1 Comparing with another method

We prepare two methods as comparison objects: The *Original* method extracted features from the whole image and the *FRI-comb* method extracted features from only feature region images obtained by auto-extraction method. For the *Original* and the *FRI-comb*, we set parameters corresponding to the best accuracy for each method. In the *Original*, for description of SIFT, we set the interval is 20px and the description area is 31[px]×31[px]. In the *FRI-comb*, we calculate the SIFT by three type conditions: the description area is 31[px]×31[px], 51[px]×51[px], and 71[px]×71[px], and the interval is 20[px], 25[px] and 35[px].

We need two types of supervised data for our method. Therefore, 60% of datasets is supervised data in the 1st step, 20% of datasets is supervised data in 2nd step and the rest of datasets is test data for confirming the accuracy of our method. In the others, 80% of datasets is supervised data and the rest is test data. As the result of comparing our method, the accuracy and precisions for each class is shown in Table 2.

Table 2 The result of comparing our method

Name	Precision [%]			Accuracy [%]
	Group1	Group2	Group3	
Original	52.6	53.7	54.8	53.8
FRI-comb	36.8	62.5	87.5	65.9
2-Step Learning	62.5	79.5	84.8	78.5

Applying 2-step learning, we achieved the accuracy of 78.5%, and it is 12.6% higher than previous method. Additionally, we confirmed that precisions of our method are higher than the others. If local images obtained by raster scanning are similar to features of a certain class learned, the score has a positive value in the 1st step. However, if they are not similar to features of a certain class or not feature regions, the score has a negative value. Hence, a score-distribution obtained from local images means how many features for a certain class exist. In addition, we think that our method can decrease the influence of regions which are not suitable for learning such as the circle in Fig.2 by calculating the statistical value from a score-distribution. Thus, our method is better than the others because it covers regions besides feature regions and saves a lot of necessary information for identification.

4.2 Investigation of generalization ability

We investigate the generalization ability of our method by exchanging train data and test data at random. Here, we exchange these data 10 times and verify it by using mean-accuracy. At this time, 60% of datasets is supervised data in the 1st step, 30% of datasets is supervised data in the 2nd step and the rest is test data. It is shown in Fig.6. This result is shown in Table 3.

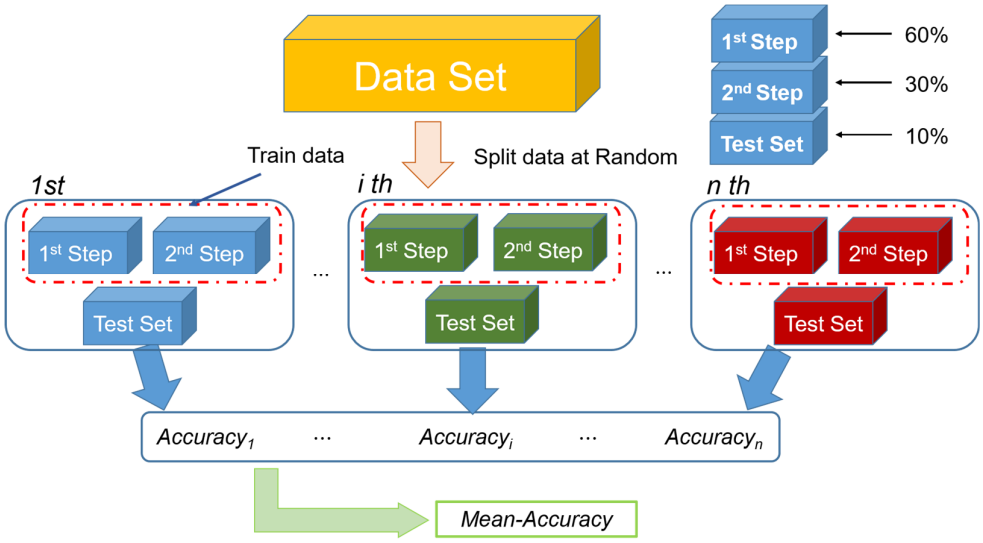

Fig.6 Exchanging train data and test data at random

Table 3 The result of investigation

Name	Mean-Precision [%]			Mean-Accuracy [%]
	Group1	Group2	Group3	
2-Step Learning	24.0	86.6	85.0	72.9

Table3 shows that our method could classify with mean-accuracy of 72.9%. However, mean-precision of Group1 was 24.0%, and this is low value. In 10 times learning, examples of normal or abnormal status are shown in Table 4.

Table 4 Examples of normal or abnormal status in the 2nd step

Status	Precision [%]			Accuracy [%]
	Group1	Group2	Group3	
Normal	73.7	84.6	66.7	75.8
Abnormal	0.0	84.2	90.9	68.9

In abnormal status, Group1 could not be classified. To verify the causing, we introduce the Recall ratio. The Recall ratio means how accurately the boundary can determine the data which belongs to a certain class. In Table 5, it is shown that verifying the Recall ratio of normal or abnormal status in 1st step by using feature region images which are not used these learning.

Table 5 Examples of normal or abnormal status in the 1st step (Recall)

Status	Recall [%]			Accuracy [%]
	Group1	Group2	Group3	
Normal	39.0	53.9	53.3	51.2
Abnormal	29.7	51.7	53.6	48.5

The result shows that normal status is about 9.3% higher than the other one. Therefore, we think that our learning about Group1 is not enough. Regarding this issue, we think the dataset with deviation affects our learning. Here, we fix the number of each class to 96 and we obtain the result of following such as Table 6.

Table 6 The result of fixing the number of each class

Name	Mean-Precision [%]			Mean-Accuracy [%]
	Group1	Group2	Group3	
2-Step Learning	84.5	53.6	87.6	75.3

Comparing the result of Table 6 with the result of Table 3, the precision of Group 1 is improving, and the precision of Group 2 is worsening. Therefore, we think Group 1 and Group 2 are in the relationship of trade-off because precision of two classes affect the number of images.

5. Conclusion

In this paper, we propose 2-step learning applying foot process region images of glomerular epithelial cell, and we validate the effectiveness of our method by two ways as follows. One is to compare with previous method. Our method achieved the accuracy of 78.5% that is higher than previous ones. The other is to investigate the generalization ability. As the result of validating it, we confirmed generalization ability by improving datasets with deviation. However, we think that Group 1 and Group 2 are in the relationship of trade-off, thereby it is difficult to improve the accuracy both Group 1 and Group 2.

Our future task is to reselect the statistical value extracted in the 2nd step. We expect the improving accuracy by selecting the statistical value which optimized because the precision of the 1st step affects score distribution.

In this study, there is a lot of tasks except it. However, we confirmed the effectiveness of our method because the accuracy of it is higher than previous method.

This paper is revised the proceedings of ICTSS 2018 [9] for the full-paper.

Appendix

Here, we explain the Fisher Vector. The details of information on the Fisher Vector are described in [5, 6, 7, 8]. It is a high dimensional vector that means the average, the variance and the burden ratio for luminance gradient vector. We can calculate it by three steps as follows.

First, we extract luminance gradient vectors from an image by SIFT. The Scale Invariant Feature Transform (SIFT) is kind of local features. In this paper, we determine to describe features on gridded points such as Fig.7.

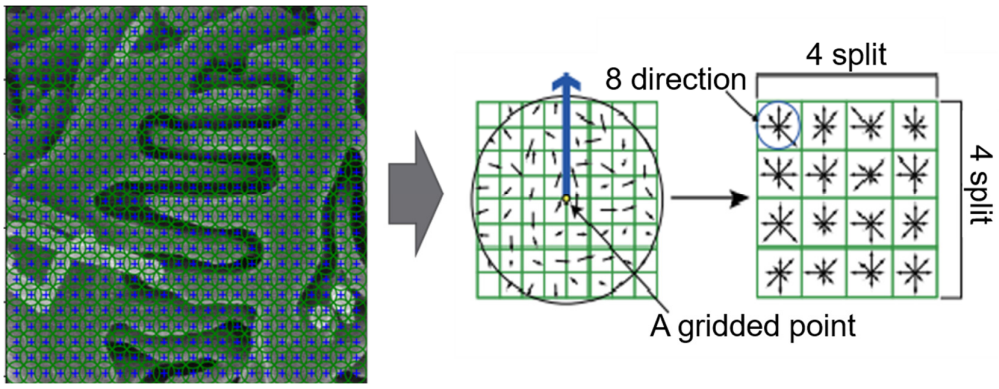

Fig.7 Describing features on gridded points (SIFT)

Moreover, we determine the scale σ which satisfied with Eq. (1) from the size of description area, where w is the size of description area.

$$w = 2\text{ceil}(3\sigma) + 1 \tag{1}$$

Second, we estimate a generation model of gradient vector by gaussian mixture model (GMM). GMM is expressed by calculating the sum of multiple gaussian distribution such as Eq. (2), where $p(\boldsymbol{x})$ is the probability distribution and π is the burden ratio.

$$p(\boldsymbol{x}) = \sum_{k=1}^{K} \pi_k p_k(\boldsymbol{x}) \tag{2}$$

Finally, the Fisher Vector is calculated by next formulas Eq. (3) – Eq. (5). These formulas mean as follows: Eq. (3) is about the burden ratio, Eq. (4) is about the average and Eq. (5) is about the variance,

$$\mathcal{G}_{\pi_k} = \frac{1}{\sqrt{\pi_k}} \sum_{t=1}^{T} (\gamma_{tk} - \pi_k) \tag{3}$$

$$\boldsymbol{\mathcal{G}_{\mu_k}} = \frac{1}{\sqrt{\pi_k}} \sum_{t=1}^{T} \gamma_{tk} \left(\frac{\boldsymbol{x_t} - \boldsymbol{\mu_k}}{\boldsymbol{\sigma_k}} \right) \tag{4}$$

$$\boldsymbol{\mathcal{G}_{\sigma_k}} = \frac{1}{\sqrt{2\pi_k}} \sum_{t=1}^{T} \gamma_{tk} \left[\frac{(\boldsymbol{x_t} - \boldsymbol{\mu_k})^2}{\boldsymbol{\sigma_k^2}} - 1 \right] \tag{5}$$

where $\boldsymbol{\mathcal{G}}$ is the Fisher Vector, γ is the posterior probability, π is the burden ratio, μ is the average, σ is the variance and T is the total of the number of gradient vectors. The dimension of the Fisher Vector is (2D+1) K, where K is the number of components of GMM and D is the dimension of SIFT.

References

[1] K. Asanuma, "Molecular biology of podocyte", ***Juntendo Medical***, Vol. 53 pp. 11-19, 2007.

[2] S. Motokawa, T. Matsuura, T. Aoki, "Extract Cell Body Region from Microscopic Image of Podocyte and a Trial of Discrimination of Cellular Degeneration by Signal Regulatory Protein α and Diabetes Mellitus", ***Med. Imag. Tech.***, Vol. 33, No. 5, pp. 208-216, 2015.

[3] Y. Ono, T. Matsuura, T. Matsuzaki, et al., "Detection of modifications in podocytes and diagnosis of kidney disease stages from SEM of podocyte cells", ***4th International Symposium of Gunma University Medical Innovation*** (Maebashi, Japan) Nov. 2017.

[4] S. Motokawa, T. Matsuura, T. Matsuzaki, et al., "A Method for Automation of Extracting Foot Process Region from Podocyte Image", ***3rd International Symposium of Gunma University Medical Innovation and 8th International Conference on Advanced Micro-Device Engineering*** (Kiryu, Japan) Dec. 2016.

[5] J. Sanchez, F. Perronnin, T. Mensink, et al., "Image Classification with the Fisher Vector: Theory and Practice", ***International Journal of Computer Vision***, Vol. 105, No.3, pp.222-245, 2013.

[6] Daivid G. Lowe, "Distinctive Image Features from Scale-Invariant Keypoints", ***International Journal of Computer Vision***, Vol. 60, No.2, pp.91-110, 2004.

[7] H. Fujiyoshi, "Gradient-Based Feature Extraction –SIFT and HOG-", ***CVIM***, Vol. 160, pp. 211-224, 2007.

[8] C. M. Bishop, "Mixtures of Gaussians" in ***Pattern Recognition and Machine Learning***, Springer, 2006, pp.430-432.

[9] Y. Ono, T. Matsuura, T. Matsuzaki, et al., "Investigation of generalization ability by applying 2-Step Learning for Glomerular Epithelial cell images", ***International Conference on Technology and Science 2018*** **(**Kiryu, Japan) Apr. 2018.

[10] S. Takahashi, M. Tomioka, K. Hiromura, et al., "SIRPα signaling regulates podocyte structure and function", ***Am. J. Physiol. Rental. Physiol.***, Vol. 305, pp.861-870, 2013.